Organic & Biomolecular Chemistry

ROYAL SOCIETY OF CHEMISTRY

PAPER

View Article Online
View Journal | View Issue

Cite this: *Org. Biomol. Chem.*, 2026, **24**, 1033

Regioselective multicomponent synthesis of α-boryl ureas: discovery of a potent main protease inhibitor

Yusif I. Gyasi,†[a] Satyanarayana Nyalata,†[a] Sophea Pa,[a] Disni Gunasekera,[a] Veerabhadra R. Vulupala,[a] Nagarjun R. Mallampudi,[a] Gopal R. Ramidi[a] and Shiqing Xu *[a,b]

Received 24th November 2025,
Accepted 27th December 2025

DOI: 10.1039/d5ob01846c

rsc.li/obc

The development of efficient synthetic methods for α-boryl ureas is of significant interest due to their potential as drug-like scaffolds in medicinal chemistry. Herein, we present a multicomponent strategy that transforms α-haloboronates, trimethylsilyl isocyanate, sodium iodide, and amines into diverse drug-like scaffold α-boryl ureas under mild conditions. This protocol features broad substrate scope and great functional-group tolerance, and enables the regioselective synthesis of previously inaccessible α-boryl ureas, including late-stage functionalization of drug molecules. Mechanistic studies suggest that a regioselective 1,2-boronate migration pathway may underlie the different regioselectivities observed with primary and secondary amines. To highlight the potential of this methodology in drug discovery, an α-boryl urea analog of nirmatrelvir was synthesized, exhibiting remarkable inhibitory activity (IC_{50} = 12 nM) against the SARS-CoV-2 main protease. This work not only provides a streamlined and practical synthetic route to diverse α-boryl ureas, but also underscores their potential as valuable scaffolds in the development of new therapeutics.

Introduction

Organoboron compounds constitute a highly versatile and widely utilized class of reagents in organic synthesis and catalysis.[1–7] Their unique chemical properties, including high functional-group tolerance, stability, and generally low toxicity, have made them indispensable tools for chemists. Landmark transformations such as hydroboration[8,9] and the Suzuki–Miyaura coupling[1–3] have profoundly shaped modern synthetic methodologies. Beyond these classic reactions, the 1,2-migration of boronate-ate complexes has emerged as one of the most valuable transformations in boron chemistry for organic synthesis.[10–14] Typically, these transformations begin with the addition of a nucleophile to the boron atom, forming sp^3-hybridized boronate-ate complexes. These complexes readily undergo the 1,2-migration of a boron-substituent to an α-carbon, facilitated by factors such as α-leaving group,[12,15–17] α-boryl radical,[10,11] or electrophilic activation of an alkenyl boronate complex.[7,12,14] In addition to their remarkable synthetic utility, boron-containing compounds have recently garnered significant interest in chemical biology and drug discovery.[18–29] The distinctive electronic properties of boron, particularly its vacant p-orbital, enable reversible covalent interactions with biological nucleophiles such as hydroxyl and amine groups found in enzymes, carbohydrates, and nucleic acids. This enables the formation of anionic sp^3-hybridized complexes. The ability to form dynamic sp^3-hybridized anionic complexes, combined with the hydrogen-bonding potential of boronic acids, makes boron an exceptional element for designing drugs that can anchor to biological targets with high specificity and affinity. Among boron-based scaffolds, α-aminoboronic acids and esters stand out due to their unique structural and functional properties, serving as bioisosteres of amino acids and versatile pharmacophores in biologically active agents and molecular probes.[22,23,30,31] α-Aminoboronic acids and esters have proven to be key pharmacophores in biologically active molecules and FDA-approved drugs, such as the proteasome inhibitors bortezomib and ixazomib citrate (Scheme 1A).[22,32–35] These breakthroughs have led to increased interest in the design of α-aminoboronic acids and esters for therapeutics.

Ureas, on the other hand, are essential structural motifs commonly found in numerous natural products and bioactive molecules, including a variety of approved therapeutics.[36–38] Notably, ureas are extensively used as peptide bond surrogates in medicinal chemistry due to their enhanced resistance to

[a]*Department of Chemistry, Texas A&M University, College Station, Texas 77843, USA. E-mail: shiqing.xu@tamu.edu*
[b]*Department of Pharmaceutical Sciences, Irma Lerma Rangel College of Pharmacy, Texas A&M University, College Station, Texas 77843, USA*
†These authors contributed equally to this work.

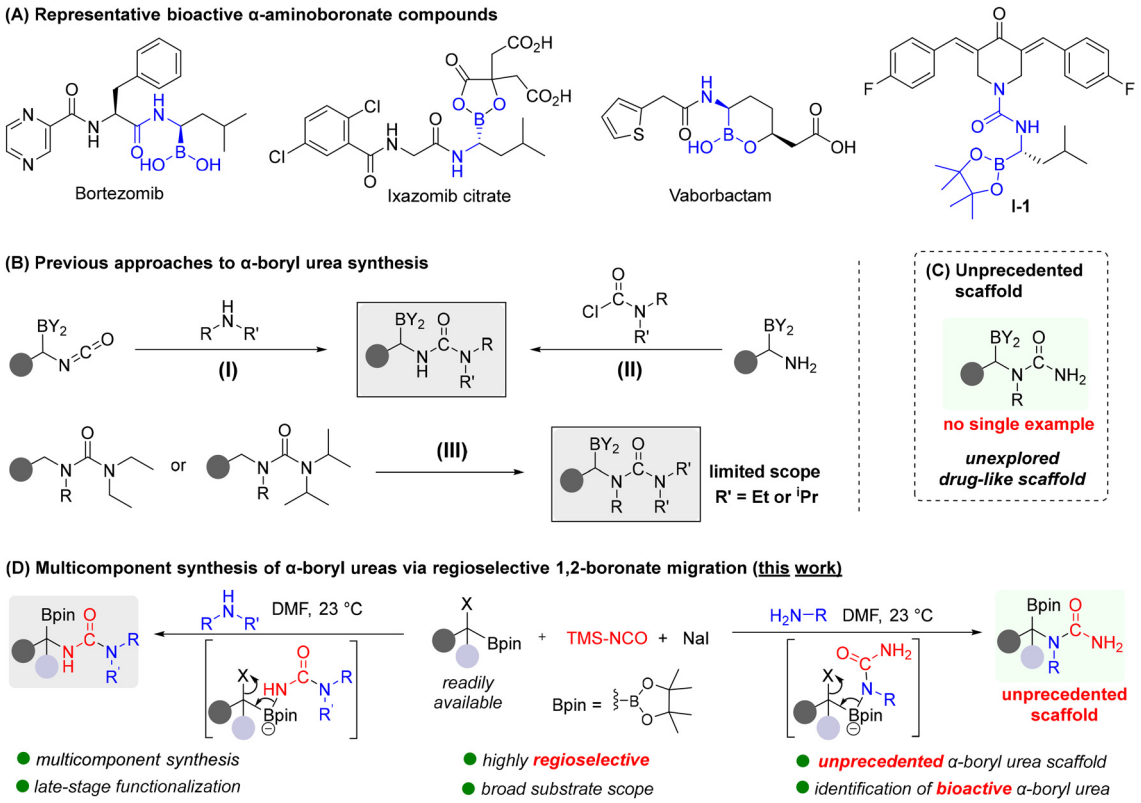

Scheme 1 (A) Representative bioactive α-aminoboronate compounds; (B) previous approaches to α-boryl urea synthesis; (C) representative unprecedented α-boryl urea scaffold; and (D) regioselective multicomponent synthesis of α-boryl ureas.

protease degradation and capability to form hydrogen bonding through the carboxyl group and the backbone *NH* moiety. By integrating the unique features of α-aminoboronates and urea pharmacophores, α-boryl ureas offer great potential as boron-containing drug-like scaffolds in drug discovery.[34,35] Thus, substantial efforts have been made to develop synthetic methods for construction of drug-like α-boryl ureas. One common approach involves the nucleophilic addition of amines to α-boryl isocyanate intermediates, which efficiently installs the urea functionality adjacent to the boryl group (Scheme 1B-I).[39–41] These α-boryl isocyanates are synthesized *via* either Curtius rearrangement of transient boroalkyl acyl azides or through [3,3]-sigmatropic rearrangement of boronated allylcyanates. Another strategy is to react with α-amino boronic esters with carbamoyl chlorides or isocyanates (Scheme 1B-II).[35] In addition, C–H borylation of ureas bearing directing groups has been employed to generate α-boryl ureas, either through borylation of α-lithiated *N*-benzylic urea[42] or *via* iridium-catalyzed C–H borylation[43,44] (Scheme 1B-III). However, these approaches require directing groups such as *N*,*N*-diethylcarbamoyl or *N*,*N*-diisopropylcarbamoyl to achieve borylation which substantially restricts the substrate scope. Despite these advances, existing synthetic methods face challenges, such as narrow substrate scope, modest functional group tolerance, and the need for multistep preparation of starting materials, which collectively hinder the efficient synthesis of more diverse α-boryl ureas and unprecedented scaffolds (Scheme 1C).

Herein, we report a new, efficient multicomponent strategy for the synthesis of α-boryl ureas. Our strategy leverages multicomponent reactions of α-haloboronates, trimethylsilyl isocyanate, sodium iodide, and diverse amines, facilitating the formation of α-boryl ureas *via* 1,2-boronate migration under mild conditions. This new approach eliminates the need for strong acid/base and pre-installation of α-boryl isocyanates and α-amino boronates that could compromise functional group compatibility, chemoselectivity, and step-efficiency (Scheme 1D). Given the broad accessibility of α-haloboronates *via* various concise synthetic routes,[45–51] this multicomponent approach would offer a highly adaptable and efficient platform. We anticipate that this methodology would dramatically expand the chemical space of α-boryl ureas, enabling streamlined access to a broad range of novel drug-like scaffolds with significant potential for medicinal chemistry applications.

Results and discussion

To test our hypothesis, we initiated investigations into the synthesis of α-boryl ureas using readily accessible α-haloboronic pinacol esters as starting materials. As a model substrate, we selected α-chloroboronate **1a**, which was conveniently syn-

thesized through Cu-catalyzed deoxygenative haloboration of 3-phenylpropanal.[51] This method provides a straightforward and efficient route to diverse secondary α-haloboronates and tertiary α-haloboronates from aldehydes and ketones. Trimethylsilyl isocyanate (TMS-NCO) was chosen as the nucleophilic isocyanate reagent.[52,53] In our initial experiment, α-chloroboronate **1a** was treated with TMS-NCO (**2**, 1.0 equiv.) in DMF at 23 °C, followed by the addition of benzylamine (**3**, 1.5 equiv.). The reaction yielded the desired α-boryl urea **4** in 5% yield (Table 1, entry 1). The major side product was benzylurea, which arose from the direct reaction of unreacted TMS-NCO **2** with benzylamine **3**, indicating sluggish formation of the α-boryl urea under these conditions. To address this limitation, we introduced sodium iodide (NaI, 1.0 equiv.) as an additive that could convert α-chloroboronate **1a** to its iodide analog to promote the reaction. This modification improved the yield of α-boryl urea **4** to 45% (entry 2). Encouraged by this result, we further optimized the reaction by increasing the amount of TMS-NCO to 1.5 equivalents. α-Boryl urea **4** was obtained at room temperature in an improved isolated yield of 66% (entry 3), highlighting the effectiveness of this strategy under mild reaction conditions. However, reducing the amount of NaI from 1.0 equivalent to 0.5 equivalent resulted in a lower yield of 41% (entry 4). We also evaluated alternative additives, including KI, TBAI, and TBAB, but none proved as effective as NaI (entries 5–7). Furthermore, we explored the influence of solvents on the reaction outcome. The reactions conducting in THF, MeCN, and DMAc afforded α-boryl urea **4** in 5%, 38%, and 56%, respectively (entries 8–10). These results suggest that polar solvents are generally favorable for this transformation. Finally, increasing the amount of benzylamine to 2.0 equivalents did not significantly improve the yield (entry 11). The structure of α-boryl urea **4** was unambiguously confirmed *via* X-ray crystallography (CCDC 2476078), providing definitive structural evidence for this new class of compounds. Notably, the regioisomeric urea **4′** was not observed in the reaction, underscoring the high regioselectivity of the transformation. This observation strongly suggests that the reaction does not proceed *via* an α-boryl isocyanate intermediate.

Table 1 Optimization of the regioselective synthesis of α-boryl urea **4** *via* α-chloroboronate **1a**

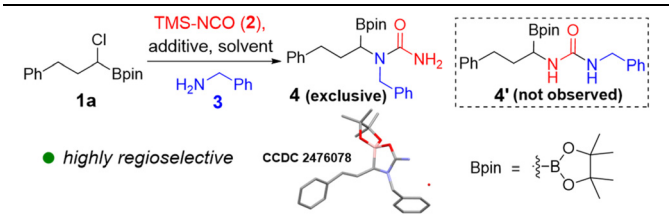

Entry	TMS-NCO **2** (equiv.)	Solvent	Additive (equiv.)	Amine **3** (equiv.)	Yield of **4** [a] (%)
1	1.0	DMF	None	1.5	5
2	1.0	DMF	NaI (1.0)	1.5	45
3	1.5	DMF	NaI (1.0)	1.5	69 (66)[b]
4	1.5	DMF	NaI (0.5)	1.5	41
5	1.5	DMF	KI (1.0)	1.5	43
6	1.5	DMF	TBAI (1.0)	1.5	32
7	1.5	DMF	TBAB (1.0)	1.5	22
8	1.5	THF	NaI (1.0)	1.5	5
9	1.5	MeCN	NaI (1.0)	1.5	38
10	1.5	DMAc	NaI (1.0)	1.5	56
11	1.5	DMF	NaI (1.0)	2.0	70

Reaction was carried out using **1a** (0.2 mmol, 1.0 equiv.), TMS-NCO, additive in solvent (0.4 mL) at 23 °C. Then benzylic amine **3** was added, and the reaction mixture was stirred for 12 h at 23 °C. [a] NMR yield using 1,3,5-trimethoxybenzene as internal standard. [b] Isolated yield. TBAI = tetrabutylammonium iodide; TBAB = tetrabutylammonium bromide; DMF = dimethylformamide; THF = tetrahydrofuran; MeCN = acetonitrile; DMAc = dimethylacetamide.

With optimized conditions in hand, we evaluated the versatility and robustness of this new protocol by synthesizing 40 unprecedented α-boryl ureas using a variety of primary amine nucleophiles and α-haloboronic pinacol esters. This systematic evaluation demonstrated the broad substrate scope and functional group tolerance of the method, which is critical for its application in medicinal chemistry. Our investigation began by assessing the reactivity of various primary amine nucleophiles, revealing significant substrate diversity (Scheme 2). A range of benzylamines, including those with electron-withdrawing and electron-donating substituents, as well as allylic amines, were compatible with the transformation, providing the corresponding α-boryl ureas **4–10** in good yields. Heterobenzylic amines such as 2-picolylamine and (2-chlorothiazol-5-yl) methanamine, which are often found in bioactive molecules, also reacted efficiently to furnish α-boryl ureas **11–14** in good yields. The scope was further extended to include a variety of alkyl amines with different functional groups, delivering various α-boryl ureas **15–26**. Notably, tryptamine, which contains an unprotected indole group that could potentially compete in side reactions, underwent selective conversion to the desired α-boryl urea **23** in 68% yield. In addition, the *NH*Boc group (*e.g.* **8**, **25**, **27**) is also compatible with no observable competing side reactions. The applicability of the method to complex molecules was also evaluated, demonstrating its utility in synthesizing derivatives of biologically relevant scaffolds. For example, amino acid derivatives and the complex drug molecule linagliptin were readily converted to their α-boryl urea analogs **27–29**. This result is particularly significant, as it highlights the potential of this method for late-stage functionalization of pharmaceuticals, a critical step in drug optimization and diversification. Aryl amine also delivered the desired α-boryl urea **30** in 57% yield. However, electron-deficient aryl amines did not undergo under the standard conditions (Fig. S2), possibly due to reduced nucleophilicity.

Next, we explored the scope of α-haloboronates for the synthesis of α-boryl ureas, further demonstrating the versatility and applicability of this novel protocol (Scheme 3). Various α-haloroboronates were readily synthesized through Cu-catalyzed deoxygenative haloroboration of cheap and commercially available aldehydes and ketones.[51] α-Boryl ureas **31–33**, and **41** were readily synthesized from alkyl α-chloroboronates using the standard conditions. Beyond alkyl α-haloboronates, we turned our attention to benzylic α-haloboronates, which could

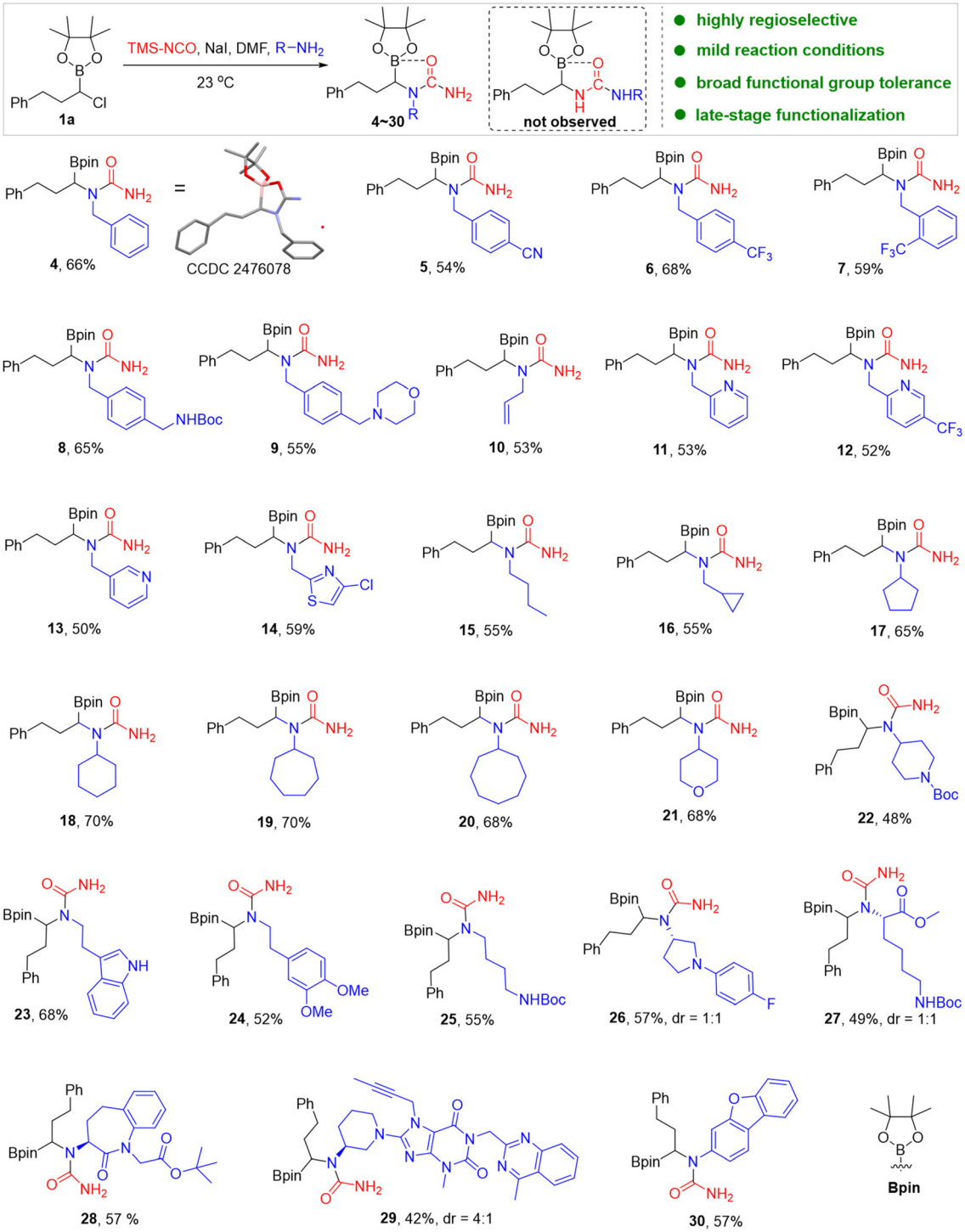

Scheme 2 Substrate scope of primary amines. Reaction was carried out using **1a** (0.5 mmol, 1.0 equiv.), TMS-NCO (1.5 equiv.), NaI (1.0 equiv.) in DMF (1 mL) at 23 °C. Then primary amine (1.5 equiv.) was added, and the reaction mixture was stirred for 6–16 h. All yields and diastereomeric ratios (dr) are for isolated α-boryl urea products.

offer unique reactivity due to the electronic influence of the benzylic position. Notably, benzylic α-haloboronates bearing electron-withdrawing groups such as trifluoromethyl (CF_3), F, and Br, proved highly effective in this transformation, delivering diverse benzylic α-boryl ureas **34–38**. Primary alkyl amines and aryl amines such as 5-aminobenzothiazole afforded α-boryl ureas **34–38** in good yields. In addition, benzylic α-chloroboronate with electron-donating methoxy (OMe) group, was also compatible, producing the corresponding α-boryl ureas **39** and **40** in good yields. Notably, substrates

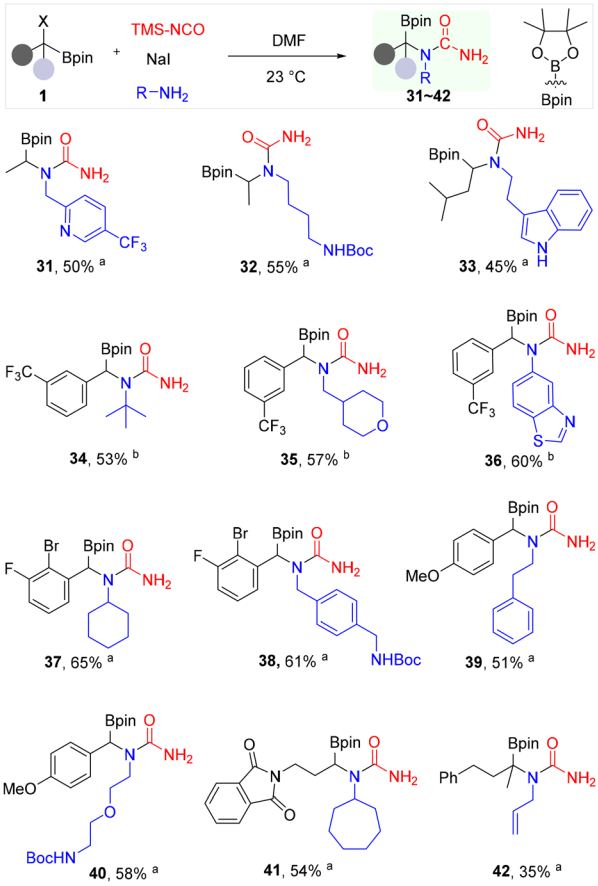

Scheme 3 Substrate scope of α-haloboronates and primary amines. Reaction was carried out using **1** (0.5 mmol, 1.0 equiv.), TMS-NCO (1.5 equiv.), NaI (1.0 equiv.) in DMF (1 mL) at 23 °C. Then primary amine (1.5 equiv.) was added, and the reaction mixture was stirred for 6–16 h. [a] X = Cl; [b] X = Br. All yields are for isolated α-boryl urea products.

with other nucleophilic functional groups such as *NH*Boc group, indole, pyridine (*e.g.* **31–33**, **38**, **40**) are compatible with no observable competing side reactions. However, the reaction of chiral α-chloroboronate under the standard conditions produced a diastereomeric mixture of α-boryl ureas (dr = 1 : 1) (Fig. S3). This observation is consistent with the reported racemization of chiral α-chloroboronates upon treatment with TMSI or NaBr.[51]

Encouraged by the successful synthesis of various monosubstituted α-boryl ureas, we set out to tackle the more demanding preparation of α,α-disubstituted derivatives, aiming to further expand the chemical diversity accessible through this protocol. In the previous elegant method,[39] the synthesis of α,α-disubstituted boryl ureas involves a multi-step sequence starting with a monosubstituted α-boryl aldehyde, followed by palladium-catalyzed α-allylation, oxidation to the corresponding α,α-disubstituted aminoboronic acid, Curtius rearrangement, and subsequent urea formation. While this strategy demonstrated the effective construction of such a scaffold, it is primarily limited to allylic-substituted boryl ureas and necessitates multiple synthetic steps. The present protocol offers a streamlined and direct approach to α,α-disubstituted boryl ureas. By employing a readily available tertiary α-chloroboronate as the starting material, we successfully synthesized the α,α-disubstituted α-boryl urea **42** in 35% yield *via* a single step. This approach offers highly efficient and regioselective synthesis of previously inaccessible α-boryl ureas and demonstrates remarkable generality by accommodating a wide variety of α-haloboronates and primary amines under mild reaction conditions.

Next, we explored the reactions using secondary amines under the standard reaction conditions. Both cyclic and acyclic secondary amines delivered corresponding α-boryl ureas **43–46** (Scheme 4). In general, reactions with secondary amines proceeded more sluggishly and afforded lower yields compared to those with primary amines. The structure of the α-boryl urea **43** was unambiguously confirmed by X-ray crystallography (CCDC 2476117), providing structural evidence for a distinct regioselectivity relative to the reactions with primary amines.

To gain mechanistic insight into the regioselective formation of α-boryl ureas from α-haloboronates and primary amines, we conducted several experiments that revealed mechanistic clues. First, replacing α-chloroboronate with 2-chlorobutane in the reaction with primary amine **47** under standard conditions produced no urea product **48**, indicating that the boron moiety is essential for this transformation (Scheme 5A). Next, reacting α-chloroboronate **1a** with TMS-NCO in the presence of the radical scavenger TEMPO (2 equiv.) under standard conditions furnished the desired α-boryl urea **6** in 65% yield, with no observable impact on the reaction efficiency (Scheme 5C). This result suggests that a radical pathway is not favoured. We then considered whether high regioselectivity with primary amines could arise from an α-aminoboronate intermediate. In this scenario, α-chloroboronates would first react with primary amines to

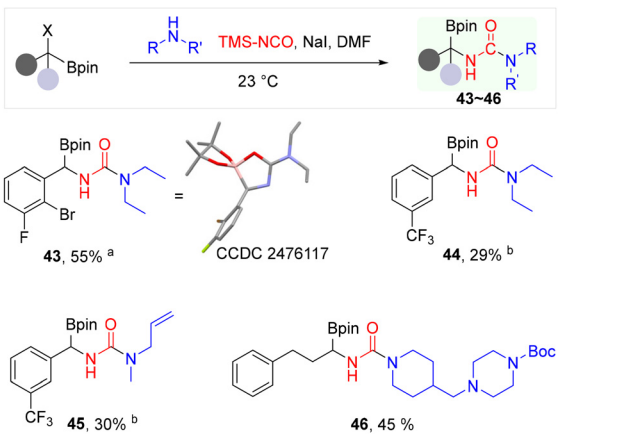

Scheme 4 The synthesis of α-boryl ureas using α-haloboronates and secondary amines. Reaction was carried out using **1** (0.5 mmol, 1.0 equiv.), TMS-NCO (1.5 equiv.), NaI (1.0 equiv.) in DMF (1 mL) at 23 °C. Then secondary amine (1.5 equiv.) was added, and the reaction mixture was stirred for 12–24 h. [a] X = Cl; [b] X = Br. All yields are for isolated α-boryl urea products.

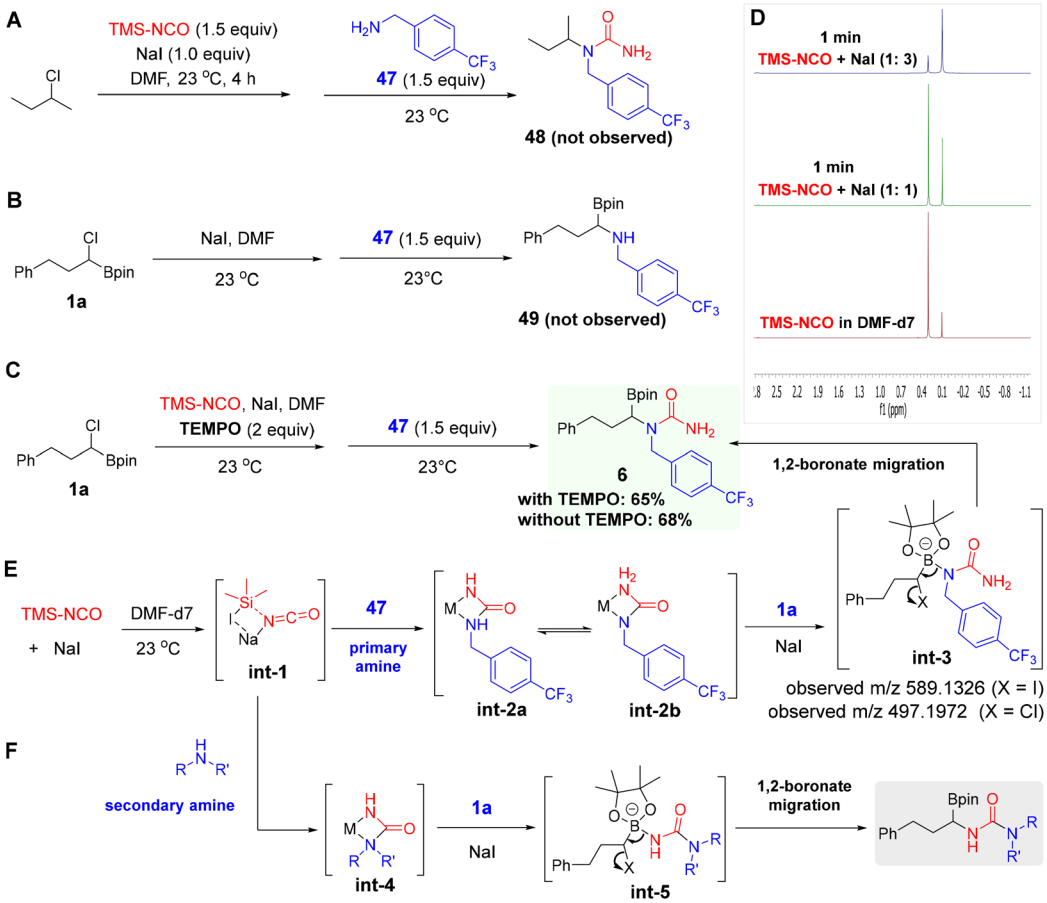

Scheme 5 (A) Control experiment using 2-chlorobutane under standard conditions; (B) control experiment of **1a** conducted in the absence of TMS-NCO; (C) control experiments of **1a** conducted in the absence and presence of TEMPO; (D) ^{1}H NMR spectra of TMS-NCO, and TMS-NCO with NaI in DMF-d7; (E) proposed reaction pathway for the regioselective formation of α-boryl urea **6** from primary amine **47**; and (F) proposed reaction pathway for the formation of α-boryl ureas from secondary amines.

give α-aminoboronates, which would subsequently react with TMS-NCO to form α-boryl ureas. To test this hypothesis, we carried out a control reaction between **1a**, primary amine **47**, and NaI in DMF at 23 °C. However, α-aminoboronate **49** was not observed (Scheme 5B). To further probe the mechanism, we monitored the reaction in DMF-d7 by ^{1}H NMR spectroscopy. In the absence of NaI, the reaction progressed slowly. However, upon the addition of NaI, a new peak at a chemical shift of δ 0.1 ppm was immediately observed, distinct from the δ 0.29 ppm shift of TMS-NCO. This new δ 0.1 ppm peak was attributed to the formation of trimethylsilyl halide. To explore the role of NaI, we conducted a control experiment by mixing TMS-NCO and NaI, which also immediately exhibited the appearance of the peak at δ 0.1 ppm, providing evidence for the generation of a new isocyanate species, designated as **int-1** (Scheme 5D). This observation aligns with previous reports where TMS-NCO was shown to react with beryllium chloride ($BeCl_2$) and gallium chloride ($GaCl_3$).[54,55] Based on these observations, plausible mechanistic pathways are proposed to rationalize the observed distinct regioselectivity profiles of primary *versus* secondary amines.

The reaction may begin with the formation of nucleophilic isocyanate species **int-1** *via* interaction of TMS-NCO with NaI. This intermediate **int-1** reacts with primary amine to produce urea intermediates **int-2a** and **int-2b** through a reversible manner. *N*,*N*-Disubstituted species **int-2b** reacts with α-chloroboronate to form boron-ate complex **int-3**, which then undergoes a rapid and regioselective 1,2-boronate rearrangement to generate the desired product **6**. In contrast, **int-2a** containing an *NH*-M moiety, as previously reported, would exhibit less favorable 1,2-boronate migration compared to *N*,*N*-disubstituted **int-2b**.[56] The formation of boron-ate complexes **int-3** was supported by high-resolution mass spectrometry analysis (Scheme 5E and Fig. S1). When **int-1** reacts with a secondary amine, only a single urea intermediate **int-4** is formed, which subsequently reacts with α-chloroboronate to yield α-boryl ureas *via* a comparatively sluggish 1,2-boronate migration (Scheme 5F).

To further demonstrate the versatility of our methodology and the potential of α-boryl ureas in drug discovery, we designed and synthesized an α-boryl urea analog of nirmatrelvir, designated as compound **51**. Nirmatrelvir, an orally avail-

able SARS-CoV-2 main protease (MPro) inhibitor developed by Pfizer represents a significant breakthrough in antiviral drug development.[57] MPro is a SARS-CoV-2 essential protease that plays pivotal roles in viral replication and pathogenesis. MPro tends to be highly conserved among various coronaviruses (CoVs) and there is no similar human protease, making it one of the most attractive drug targets for developing broad-spectrum antivirals against coronaviruses.[58–61] MPro is a cysteine protease with three domains, and its active form is a homodimer comprising two protomers. Each protomer contains a Cys145-His41 catalytic dyad, where cysteine serves as the nucleophile in the proteolytic process.[62] Nirmatrelvir is covalent MPro inhibitor *via* its distinctive nitrile warhead to interact with catalytic Cys145.[57] In addition, nirmatrelvir's trifluoromethyl amide moiety at the P4 position plays an important role in its binding affinity to MPro. The amide nitrogen forms a hydrogen bond with the backbone carbonyl oxygen of E166, while the trifluoromethyl group engages in additional hydrogen bonding interactions with Q192 and a water molecule, further stabilizing the inhibitor-protease complex.[57] Since the onset of the COVID-19 pandemic in 2020, we have developed many covalent MPro inhibitors.[63–67] To continue the MPro inhibitor development, we sought to explore whether replacing the trifluoromethyl amide group of nirmatrelvir with an α-boryl urea moiety at the P4 position could provide enhanced binding interactions with MPro. Compound **51** was synthesized using our novel approach, starting from α-chloroboronate **1b** and amine **50** (Scheme 6A). Remarkably, compound **51** exhibited exceptional inhibitory activity against MPro, achieving an IC_{50} value of 12 nM by the previously reported assay,[68] which is approximately three times more potent than nirmatrelvir (Scheme 6B). This result underscores the potential of the α-boryl urea moiety to enhance binding affinity and potency against enzymatic targets in drug discovery.

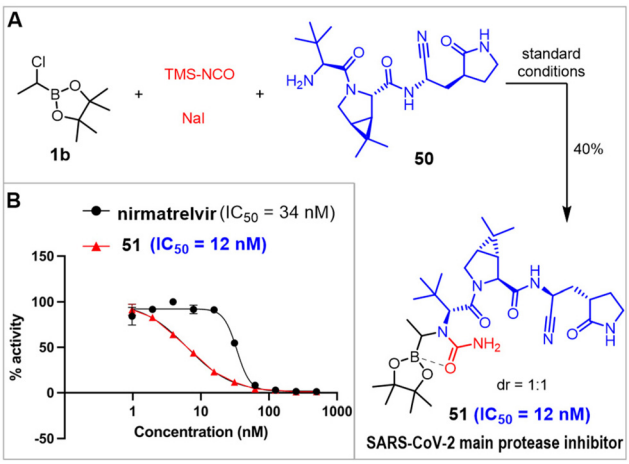

Scheme 6 (A) Synthesis of nirmatrelvir analog α-boryl urea **51**; (B) inhibition curves of nirmatrelvir and **51** on the SARS-CoV-2 MPro. Triplicate experiments were performed for each compound. For all experiments, 20 nM MPro was incubated with an inhibitor for 30 min before 10 μM Sub3 was added. The MPro-catalyzed Sub3 hydrolysis rate was determined by measuring linear increase of product fluorescence (Ex: 336 nm/Em: 455 nm) for 5 min. The IC_{50} for **51** was 12.5 ± 1.7 nM and nirmatrelvir was 33.8 ± 1.1 nM.

Conclusions

In summary, we have developed a novel regioselective multicomponent synthesis of previously inaccessible α-boryl ureas through the reaction of α-haloboronates, trimethylsilyl isocyanate, sodium iodide, and diverse amines under mild conditions. This method offers a versatile and efficient route to a broad range of α-boryl ureas, overcoming the limitations of existing multistep syntheses and narrow substrate scopes. The versatility and adaptability of this method were demonstrated through the synthesis of 40 unprecedented α-boryl ureas, encompassing a wide range of substrates, including sterically demanding and biologically relevant molecules. Plausible mechanistic pathways are proposed to rationalize the observed distinct regioselectivity of primary *versus* secondary amines, involving regioselective 1,2-boronate migration. Moreover, the potential of α-boryl ureas in drug discovery is highlighted by an α-boryl urea nirmatrelvir analog **51**, which exhibited exceptional inhibitory activity against SARS-CoV-2 main protease. Overall, this study not only offers a streamlined and practical platform for accessing diverse α-boryl ureas, but also underscores their potential as valuable scaffolds in the development of new therapeutics.

Author contributions

Y. I. G. and S. N. contributed equally to this work. Y. I. G. and S. N. contributed to conceptualization, data curation, formal analysis, investigation, methodology, validation, visualization, writing – original draft. S. P., D. G., V. R. V., N. R. M. and G. R. R. contributed to data curation, formal analysis, investigation, validation. S. X. contributed to conceptualization, funding acquisition, project administration, resources, supervision, validation, visualization, writing – review and editing.

Conflicts of interest

There are no conflicts to declare.

Data availability

Data supporting this article are available within the main text and the supplementary information (SI). Supplementary information: all experimental procedures, characterization data, and spectra supporting the findings of this study. See DOI: https://doi.org/10.1039/d5ob01846c.

CCDC 2476078 and 2476117 contain the supplementary crystallographic data for this paper.[69a,b]

Acknowledgements

This work was supported by the Welch Foundation (grant A-2174), the National Institutes of Health (grants R21AI164088 and R21AI166521), and the Department of Pharmaceutical Sciences and the Department of Chemistry at Texas A&M University. We would like to thank Dr Nattamai Bhuvanesh for X-ray crystal structure analysis.

References

1 N. Miyaura and A. Suzuki, *Chem. Rev.*, 1995, **95**, 2457–2483.
2 A. Suzuki, *Angew. Chem., Int. Ed.*, 2011, **50**, 6722–6737.
3 C. C. C. Johansson Seechurn, M. O. Kitching, T. J. Colacot and V. Snieckus, *Angew. Chem., Int. Ed.*, 2012, **51**, 5062–5085.
4 D. G. Hall, Structure, Properties, and Preparation of Boronic Acid Derivatives, in *Boronic Acids*, 2011, pp. 1–133.
5 J. W. B. Fyfe and A. J. B. Watson, *Chem*, 2017, **3**, 31–55.
6 D. Leonori and V. K. Aggarwal, *Angew. Chem., Int. Ed.*, 2015, **54**, 1082–1096.
7 S. Namirembe and J. P. Morken, *Chem. Soc. Rev.*, 2019, **48**, 3464–3474.
8 H. C. Brown and B. C. S. Rao, *J. Am. Chem. Soc.*, 1956, **78**, 5694–5695.
9 K. Burgess and M. J. Ohlmeyer, *Chem. Rev.*, 1991, **91**, 1179–1191.
10 M. Kischkewitz, F. W. Friese and A. Studer, *Adv. Synth. Catal.*, 2020, **362**, 2077–2087.
11 G. J. Lovinger and J. P. Morken, *Eur. J. Org. Chem.*, 2020, 2362–2368.
12 E.-I. Negishi and M. J. Idacavage, *Org. Chem.*, 1985, **33**, 1–246.
13 J. Tsien, C. Hu, R. R. Merchant and T. Qin, *Nat. Rev. Chem.*, 2024, **8**, 605–627.
14 H. Wang, C. Jing, A. Noble and V. K. Aggarwal, *Angew. Chem., Int. Ed.*, 2020, **59**, 16859–16872.
15 D. Leonori and V. K. Aggarwal, *Acc. Chem. Res.*, 2014, **47**, 3174–3183.
16 D. S. Matteson, *Acc. Chem. Res.*, 1988, **21**, 294–300.
17 D. S. Matteson, *J. Org. Chem.*, 2013, **78**, 10009–10023.
18 A. Adamczyk-Woźniak, K. M. Borys and A. Sporzyński, *Chem. Rev.*, 2015, **115**, 5224–5247.
19 S. J. Baker, C. Z. Ding, T. Akama, Y.-K. Zhang, V. Hernandez and Y. Xia, *Chem. Rev.*, 2009, **1**, 1275–1288.
20 S. J. Baker, J. W. Tomsho and S. J. Benkovic, *Chem. Rev.*, 2011, **40**, 4279–4285.
21 B. C. Das, P. Thapa, R. Karki, C. Schinke, S. Das, S. Kambhampati, S. K. Banerjee, P. Van Veldhuizen, A. Verma, L. M. Weiss and T. Evans, *Future Med. Chem.*, 2013, **5**, 653–676.
22 D. B. Diaz and A. K. Yudin, *Nat. Chem.*, 2017, **9**, 731–742.
23 R. J. Grams, W. L. Santos, I. R. Scorei, A. Abad-García, C. A. Rosenblum, A. Bita, H. Cerecetto, C. Viñas and M. A. Soriano-Ursúa, *Chem. Rev.*, 2024, **124**, 2441–2511.
24 P. C. Trippier and C. McGuigan, *MedChemComm*, 2010, **1**, 183–198.
25 W. Yang, X. Gao and B. Wang, *Med. Res. Rev.*, 2003, **23**, 346–368.
26 J. P. M. António, R. Russo, C. P. Carvalho, P. M. S. D. Cal and P. M. P. Gois, *Chem. Soc. Rev.*, 2019, **48**, 3513–3536.
27 S. Chatterjee, N. M. Tripathi and A. Bandyopadhyay, *Chem. Commun.*, 2021, **57**, 13629–13640.
28 B. C. Das, N. K. Nandwana, S. Das, V. Nandwana, M. A. Shareef, Y. Das, M. Saito, L. M. Weiss, F. Almaguel, N. S. Hosmane and T. Evans, *Molecules*, 2022, **27**, 2615.
29 M. Zheng, L. Kong and J. Gao, *Chem. Soc. Rev.*, 2024, **53**, 11888–11907.
30 W. Ming, H. S. Soor, X. Liu, A. Trofimova, A. K. Yudin and T. B. Marder, *Chem. Soc. Rev.*, 2021, **50**, 12151–12188.
31 S. Touchet, F. Carreaux, B. Carboni, A. Bouillon and J.-L. Boucher, *Chem. Soc. Rev.*, 2011, **40**, 3895–3914.
32 E. S. Priestley and C. P. Decicco, *Org. Lett.*, 2000, **2**, 3095–3097.
33 R. Smoum, A. Rubinstein, V. M. Dembitsky and M. Srebnik, *Chem. Rev.*, 2012, **112**, 4156–4220.
34 L.-Q. Han, X. Yuan, X.-Y. Wu, R.-D. Li, B. Xu, Q. Cheng, Z.-M. Liu, T.-Y. Zhou, H.-Y. An, X. Wang, T.-M. Cheng, Z.-M. Ge, J.-R. Cui and R.-T. Li, *Eur. J. Med. Chem.*, 2017, **125**, 925–939.
35 W. Zhang, H. Bai, L. Han, H. Zhang, B. Xu, J. Cui, X. Wang, Z. Ge and R. Li, *Bioorg. Med. Chem. Lett.*, 2018, **28**, 2459–2464.
36 A. D. Jagtap, N. B. Kondekar, A. A. Sadani and J.-W. Chern, *Curr. Med. Chem.*, 2017, **24**, 622–651.
37 A. K. Ghosh and M. Brindisi, *J. Med. Chem.*, 2020, **63**, 2751–2788.
38 R. Ronchetti, G. Moroni, A. Carotti, A. Gioiello and E. Camaioni, *RSC Med. Chem.*, 2021, **12**, 1046–1064.
39 Z. He, A. Zajdlik, J. D. St Denis, N. Assem and A. K. Yudin, *J. Am. Chem. Soc.*, 2012, **134**, 9926–9929.
40 S. Touchet, A. Macé, T. Roisnel, F. Carreaux, A. Bouillon and B. Carboni, *Org. Lett.*, 2013, **15**, 2712–2715.
41 A. Zajdlik, Z. He, J. D. St Denis and A. K. Yudin, *Synthesis*, 2014, **46**, 445–454.
42 Q. Qi, X. Yang, X. Fu, S. Xu and E.-i. Negishi, *Angew. Chem., Int. Ed.*, 2018, **57**, 15138–15142.
43 L. Chen, Y. Yang, L. Liu, Q. Gao and S. Xu, *J. Am. Chem. Soc.*, 2020, **142**, 12062–12068.
44 M. He, L.-J. Xie, L. Chen and S. Xu, *ACS Catal.*, 2024, **14**, 18701–18707.
45 T. Fang, J. Qiu, K. Yang and Q. Song, *Org. Chem. Front.*, 2021, **8**, 1991–1996.
46 F.-C. Gao, M. Li, H.-Y. Gu, X.-Y. Chen, S. Xu, Y. Wei and K. Hong, *J. Org. Chem.*, 2023, **88**, 14246–14254.
47 T. D. Ho, B. J. Lee, C. Tan, J. A. Utley, N. Q. Ngo and K. L. Hull, *J. Am. Chem. Soc.*, 2023, **145**, 27230–27235.
48 D. S. Matteson, B. S. Collins, V. K. Aggarwal and E. J. O. R. Ciganek, *The Matteson Reaction*, 2004, pp. 427–860.
49 D. S. Matteson and D. Majumdar, *J. Am. Chem. Soc.*, 1980, **102**, 7588–7590.

50 J. Schmidt, J. Choi, A. T. Liu, M. Slusarczyk and G. C. Fu, *Science*, 2016, **354**, 1265–1269.
51 D. Wang, J. Zhou, Z. Hu and T. Xu, *J. Am. Chem. Soc.*, 2022, **144**, 22870–22876.
52 S. Guo, W. Sun, J. W. Tucker, K. D. Hesp and N. K. Szymczak, *Chem. – Eur. J.*, 2023, **29**, e202203578.
53 T. Sasaki, A. Nakanishi and M. Ohno, *J. Org. Chem.*, 1981, **46**, 5445–5447.
54 C. Berthold, M. Müller, S. I. Ivlev, D. M. Andrada and M. R. Buchner, *Dalton Trans.*, 2023, **52**, 13547–13554.
55 K. Bläsing, J. Bresien, S. Maurer, A. Schulz and A. Villinger, *Eur. J. Inorg. Chem.*, 2021, **2021**, 1913–1920.
56 Q. Xie and G. Dong, *J. Am. Chem. Soc.*, 2021, **143**, 14422–14427.
57 D. R. Owen, C. M. N. Allerton, A. S. Anderson, L. Aschenbrenner, M. Avery, S. Berritt, B. Boras, R. D. Cardin, A. Carlo, K. J. Coffman, A. Dantonio, L. Di, H. Eng, R. Ferre, K. S. Gajiwala, S. A. Gibson, S. E. Greasley, B. L. Hurst, E. P. Kadar, A. S. Kalgutkar, J. C. Lee, J. Lee, W. Liu, S. W. Mason, S. Noell, J. J. Novak, R. S. Obach, K. Ogilvie, N. C. Patel, M. Pettersson, D. K. Rai, M. R. Reese, M. F. Sammons, J. G. Sathish, R. S. P. Singh, C. M. Steppan, A. E. Stewart, J. B. Tuttle, L. Updyke, P. R. Verhoest, L. Wei, Q. Yang and Y. Zhu, *Science*, 2021, **374**, 1586–1593.
58 K. Akaji, H. Konno, H. Mitsui, K. Teruya, Y. Shimamoto, Y. Hattori, T. Ozaki, M. Kusunoki and A. Sanjoh, *J. Med. Chem.*, 2011, **54**, 7962–7973.
59 J. S. Morse, T. Lalonde, S. Xu and W. R. Liu, *ChemBioChem*, 2020, **21**, 730–738.
60 S. Ullrich and C. Nitsche, *Bioorg. Med. Chem. Lett.*, 2020, **30**, 127377.
61 Y. Liu, C. Liang, L. Xin, X. Ren, L. Tian, X. Ju, H. Li, Y. Wang, Q. Zhao, H. Liu, W. Cao, X. Xie, D. Zhang, Y. Wang and Y. Jian, *Eur. J. Med. Chem.*, 2020, **206**, 112711.
62 K. Anand, J. Ziebuhr, P. Wadhwani, J. R. Mesters and R. Hilgenfeld, *Science*, 2003, **300**, 1763.
63 K. S. Yang, X. R. Ma, Y. Ma, Y. R. Alugubelli, D. A. Scott, E. C. Vatansever, A. K. Drelich, B. Sankaran, Z. Z. Geng, L. R. Blankenship, H. E. Ward, Y. J. Sheng, J. C. Hsu, K. C. Kratch, B. Zhao, H. S. Hayatshahi, J. Liu, P. Li, C. A. Fierke, C.-T. K. Tseng, S. Xu and W. R. Liu, *ChemMedChem*, 2021, **16**, 942–948.
64 Y. R. Alugubelli, Z. Z. Geng, K. S. Yang, N. Shaabani, K. Khatua, X. R. Ma, E. C. Vatansever, C.-C. Cho, Y. Ma, J. Xiao, L. R. Blankenship, G. Yu, B. Sankaran, P. Li, R. Allen, H. Ji, S. Xu and W. R. Liu, *Eur. J. Med. Chem.*, 2022, **240**, 114596.
65 Y. Ma, K. S. Yang, Z. Z. Geng, Y. R. Alugubelli, N. Shaabani, E. C. Vatansever, X. R. Ma, C.-C. Cho, K. Khatua, J. Xiao, L. R. Blankenship, G. Yu, B. Sankaran, P. Li, R. Allen, H. Ji, S. Xu and W. R. Liu, *Eur. J. Med. Chem.*, 2022, **240**, 114570.
66 Z. Z. Geng, S. Atla, N. Shaabani, V. Vulupala, K. S. Yang, Y. R. Alugubelli, K. Khatua, P.-H. Chen, J. Xiao, L. R. Blankenship, X. R. Ma, E. C. Vatansever, C.-C. D. Cho, Y. Ma, R. Allen, H. Ji, S. Xu and W. R. Liu, *J. Med. Chem.*, 2023, **66**, 11040–11055.
67 K. Khatua, Y. R. Alugubelli, K. S. Yang, V. R. Vulupala, L. R. Blankenship, D. Coleman, S. Atla, S. P. Chaki, Z. Z. Geng, X. R. Ma, J. Xiao, P.-H. Chen, C.-C. D. Cho, S. Sharma, E. C. Vatansever, Y. Ma, G. Yu, B. W. Neuman, S. Xu and W. R. Liu, *Antiviral Res.*, 2024, **225**, 105874.
68 E. C. Vatansever, K. S. Yang, A. K. Drelich, K. C. Kratch, C.-C. Cho, K. R. Kempaiah, J. C. Hsu, D. M. Mellott, S. Xu, C.-T. K. Tseng and W. R. Liu, *Proc. Natl. Acad. Sci. U. S. A.*, 2021, **118**, e2012201118.
69 (*a*) CCDC 2476078: Experimental Crystal Structure Determination, 2026, DOI: 10.5517/ccdc.csd.cc2p3khw; (*b*) CCDC 2476117: Experimental Crystal Structure Determination, 2026, DOI: 10.5517/ccdc.csd.cc2p3lr5.